Usefulness of fat-containing agents in research: an initial study of approximate bone fat content for magnetic resonance imaging

Yasuo Takatsu

yasuo.takatsu@fujita-hu.ac.jp

Fujita Health University: Fujita Ika Daigaku https://orcid.org/0000-0002-4384-089X

Hiroshi Ohnishi

Geisei Ortho Clinic

Tomoko Tateyama

Fujita Health University: Fujita Ika Daigaku

Yuriko Nohara

Osaka Medical Association

Kenichiro Yamamura

Tokushima Bunri University - Kagawa Campus: Tokushima Bunri Daigaku - Kagawa Campus

Kunihiro Yabe

Yamagata Prefectural Shinjo Hospital

Tosiaki Miyati

Kanazawa University Graduate School of Medical Sciences: Kanazawa Daigaku Daigakuin Iyaku Hokengaku Sogo Kenkyuka Iyaku Hoken Gakuiki Igakurui

Research Article

Keywords: magnetic resonance imaging, fat-containing nutrient solution, estimated fat fraction based on signal intensity, bone mineral content, bone mineral density

Posted Date: May 12th, 2023

DOI: https://doi.org/10.21203/rs.3.rs-2852198/v1

Version of Record: A version of this preprint was published at Physical and Engineering Sciences in Medicine on February 20th, 2024. See the published version at https://doi.org/10.1007/s13246-023-01372-y.

Abstract

Purpose

To investigate the usefulness of commercially available fat-containing agents in magnetic resonance imaging (MRI) based on bone mineral measurement.

Methods

The proximal femurs obtained from 14 volunteers were analyzed by 0.3T MRI with a fat-containing nutrient solution (based on soybean oil, 10% and 20%), 100% soybean oil and saline as reference substances. Fat content was estimated based on the relationship between the intensities of the signals of the reference substances. Since this was an approximate value, it was set as the estimated fat fraction based on signal intensity (SIeFF, %). The SIeFF values of the femoral bone marrow, including the femoral head, neck, shaft, and trochanter area, were measured. Reference substances were set as close as possible to the outside of both proximal femurs. MRI data were compared in terms of bone mineral content (BMC) and bone mineral density (BMD) by dual-energy X-ray absorptiometry (DXA) in the proximal femur. MRI and DXA data were obtained on the same day.

Results

According to Pearson's correlation coefficient, the SIeFF and total BMC and BMD data revealed strong and moderate inverse correlations in the femoral head ($r < -0.74$) and other sites ($r = -0.66$ to -0.45), respectively.

Conclusion

Commercially available fat-containing agents may be useful in estimating the bone marrow fat content for bone mineral measurement by MRI. SIeFF and BMC and BMD showed a strong inverse correlation in the femoral head. Nevertheless, a more thorough study is warranted before this method can be used as an alternative to DXA.

1. Introduction

Osteoporosis is a common health problem among older individuals. A decrease in bone mass is associated with an increase in the risk of fracture [1]. Therefore, early diagnosis of osteoporosis is a key to managing locomotive syndrome, particularly due to fractures in the elderly. Aging [2], diabetes [3], and obesity [4] are some of the causes of osteoporosis. In addition, it has been reported that mesenchymal stem cell differentiation is shifted to adipocytes rather than osteoblasts [5]. Other causes of osteoporosis include fat deposition in various organs and surroundings and metabolic syndrome (particularly involving body fat) [6–8]. Lack of exercise and an unbalanced diet due to aging lead to metabolic syndrome. Moreover, a decrease in bone mass is associated with an increase in bone marrow fat [9, 10].

Conventionally, dual-energy X-ray absorptiometry (DXA) has been used for the quantitative measurement of bone mass [11]. The quantitative data obtained through DXA are bone mineral density (BMD) (g/cm^2) and bone mineral content (BMC) (g). These parameters are evaluated using two-dimensional transmission images at the level of skeletal segments, the lumbar spine, hip, forearm, and whole body [11]. It has also been reported that X-ray computed tomography can be used to measure the bone marrow adipose tissue content and BMD [12].

Other methods for the measurement of fat content using a magnetic resonance (MR) system have been reported. Fat content could be calculated from opposed-phase images, which have previously shown a strong correlation with *de facto* values [13]. Moreover, it has been demonstrated that MR spectroscopy (MRS) is useful in the evaluation of osteoporosis [14, 15]. A sequence of the Dixon method, specifically for fat content measurement, has also been reported [16]. The multi-echo Dixon method with a three-dimensional-fast-field echo sequence uses multiple acquired echoes to generate water, fat, T2*, R2*, and in-phase and opposed-phase images. Multi-echo Dixon-Quant imaging has exhibited high reliability for the measurement of fat content in lumbar vertebral marrow and paraspinal muscles, and is suitable for use in clinical practice [16].

However, the above methods are characterized by limitations. X-ray methods (e.g., DXA and X-ray computed tomography) are associated with several disadvantages. The regular use of X-rays raises concerns regarding the exposure of individuals to this harmful radiation. MR methods (e.g., MR imaging [MRI] and MRS) help overcome this limitation. However, they are also characterized by disadvantages, such as the need for an additional scan for the measurement of fat content and the extra time required for this procedure, thereby prolonging the total examination time. Moreover, the sequence specialized for the measurement of fat content with MRI [16, 17] depends on the technical specifications of the MRI equipment, and is not compatible with all devices at present. In addition, the images used to measure fat content cannot be used for other diagnoses. Thus, it is necessary to shorten the time required for this examination.

Ideally, images commonly used in routine MRI examinations should be utilized for the estimation of BMC and BMD. Furthermore, the development of methods that do not rely on sequences or facilities is desirable. Therefore, we focused on using reference materials for performing routine MRI examinations to make the process independent of requiring equipment and sequences to compare signal intensity in the bone. When the fat content was estimated, a fat-containing solution as a reference substance should be used. However, the uniform emulsification of water and oil involves complicated procedures, can be challenging due to unevenness caused by air contamination, and requires the use of special chemicals and techniques [18].

Intralipos® (Otsuka Pharmaceutical Co., Ltd., Tokyo, Japan) is an easy to handle and safe off-the-shelf fat-containing solution used as a nutritional supplement [19, 20] in numerous hospitals. In addition, since it is commercially available, it can be purchased at medical and educational facilities. Similar fat-containing agents (Intralipid ®; Fresenius Kabi, Uppsala, Sweden) have been used in fat fraction studies

[21, 22]. If Intralipos® is to be contrasted with bone fat as a reference, it needs to be placed close to the bone. In the present study, we focused on the proximal femur, which is the site used for the measurement of BMD and least affected by movement. However, the usefulness of Intralipos® for the measurement of femoral fat mass has not been determined thus far.

The purpose of this study was to investigate the usefulness of commercially available fat-containing agents in MRI from the perspective of bone mineral measurement.

2. Materials and Methods

This was volunteer-based study, approved by the Ethics Committee of Geisei Orthoclinic (approval number, 201801; Aki, Kouchi, Japan). All volunteers provided written informed consent for their participation in this study.

2.1. MRI

The MRI equipment used in this investigation was AIRIS Vento LT 0.3T, body flex M coil (FUJIFILM Healthcare Corp., Tokyo, Japan). We selected a low-magnetic field device that has a low specific absorption rate and is easy to use as a health check device. Low-magnetic field devices are linked to less influence of the effect of susceptibility on the results compared with high-magnetic field devices. The sequence was set for T1-weighted image of the spin echo method used in routine examinations of the hip joint; at this setting, fat produces a bright signal that is easy to detect. The conditions of this examination were as follows: repetition time, 400 ms; echo time, 25 ms; matrix, 224 × 260 (phase × frequency); flip angle, 90°; number of signals averaged, 4; bandwidth, 10 kHz; scan time, 6 min; phase-encoding direction, right-left; field of view, 350 mm; slice thickness, 5 mm; slice gap, 1 mm; and number of slices, 14.

The proximal femur was set as the target area. Notably, it is easy to set reference substances by referring to the measurement of BMD in the proximal femur presented in the manual produced by the Japan Osteoporosis Society [23].

It is possible to image the proximal part of both thighs with MRI. Nevertheless, in this study, the left and right sides were individually imaged with the coil and the center of the magnetic field as much as possible to maximize the reliability of data acquisition.

Due to the characteristics of the coil, the sensitivity is reduced toward the edge versus the center of the coil. Therefore, it is necessary to correct the signal distribution. The body thickness of the volunteers was extracted from the localizer (positioning image) and reproduced using a spacer (sponge/cloth) centered on the phantom. Thereafter, the same sequence used in the volunteer study was utilized to take cross sections at the same locations as those of slices used in the analysis and measure the signal distribution. Sensitivity correction was performed by calculating the ratio of each pixel from the highest signal intensity and multiplying the obtained value by the image to be measured. A nickel chloride

phantom ($NiCl_2$, 18 mmol/L; NaCl, 0.5 w/v%; 212 × 212 × 370 mm [width × depth × height]; T_1 relaxation time, 87.2 ms; T_2 relaxation time, 84.7 ms) was set at the same position of the proximal femur.

2.2. DXA

MRI and DXA data were obtained on the same day; the MRI data were compared in terms of BMC and BMD. The DXA device used in this study was DPX-BRAVO (GE Healthcare, Madison, WI, USA). The method was performed under the following conditions: tube voltage, 76 kV; tube current, 50–1,500 μA; distance between X-ray focus and detector, 57 cm; distance between X-ray focus and skin, 15 cm; irradiation field diameter, 0.24 cm; and scan method, pencil beam.

2.3. Reference substances

The reference material must be versatile oil that is not characterized by separation problems, is stable, readily available, and can safely maintain its emulsified state for a long period of time. Therefore, we used a fat emulsion for intravenous injection with known fat content (Intralipos®) produced from refined soybean oil. Intralipos® 10% and 20% (the only two commercially available concentrations), refined soybean oil 100% (Kenko-sarara®; J-OIL MILLS, Inc., Tokyo, Japan) and saline (OTSUKA NORMAL SALINE, Otsuka Pharmaceutical Factory, Inc., Tokyo, Japan) were used as reference substances; they were enclosed in bottles with the following dimensions: 35 mm × 35 mm × 88 mm (width × depth × height). The relaxation time of saline, Intralipos® 10% and 20%, and Kenko-sarara® 100% solutions, was 2,231.3, 1,871.9, 1,389.6, and 113.5 ms in T_1 relaxation time, and 2,140.2, 1,068.2, 598.2, and 64.0 ms in T_2 relaxation time, respectively. Reference substances were set as close as possible to the outside of both proximal femur.

The value describing the relationship between each concentration of the reference substances and each signal intensity (confirmed by the Pearson product-moment correlation coefficient beforehand) was 0.99, displaying strong linearity.

2.4. Volunteers

A total of 14 healthy volunteers (11 males and three females; age [mean ± standard deviation]: 51.64 ± 11.86 years; height: 167.45 ± 9.19 cm; weight: 69.91 ± 16.78 kg) with no history of osteoporosis were included in the study. All volunteers stated that they were right-foot dominant.

2.5. Estimated fat fraction based on signal intensity (SIeFF, %) measurement for bone marrow fat

The signal intensity of bone marrow fat was measured through MRI. The measurement position was based on the manual for the BMD measurement of the proximal femur [24], and 87% of the femoral head was set as the radius of the region of interest (ROI). The femoral neck was defined as the narrowest part near the femoral head. The shaft region was defined from the center of the lesser trochanter to 30 mm

distal. The trochanter region was outside the intersection of the vertical line of the cervical body angle and the shaft axis of the femur. The ROI was set to as the maximum circle avoiding the cortical bone. The ROI of the reference substances was set at 75% of the cross-sectional area (approximately 663 mm^2). In addition, we used sliced images in which we could obtain the widest ROI for each part (Fig. 1).

After correcting the sensitivity of the reference substance position and the measurement position based on phantom data, the fat content was estimated by interpolation from the signal intensity of each area. Fat content was estimated based on the relationship between the signal intensities of the reference substances. Since this was an approximate value, it was set as the SIeFF (%).

SIeFF was calculated as follows:

SIeFF = (SI–intercept) / signal change per fat concentration of reference substances (%)

where SI is the mean value of signal intensity for the measurement sites (femoral head, neck, shaft and trochanter); the intercept was obtained based on the interpolated signal intensity of the reference substances (≒ signal intensity of 0% reference substance).

2.6. Comparison between the SIeFF of bone marrow fat and DXA data

The correlation between the SIeFF and BMC on three sites (femoral neck, BMC_N; shaft, BMC_S; and trochanter, BMC_T) and between the SIeFF and BMD on three sites (femoral neck, BMD_N; shaft, BMD_S; and trochanter, BMD_T) was calculated. Each BMD was automatically calculated by the DXA device; BMC divided by each area (cm^2).

The total values of BMC and BMD (BMC_{Total} and BMD_{Total}) were automatically calculated by the DXA device as follows:

$$BMC_{Total} = BMC_N + BMC_S + BMC_T$$

$$BMD_{Total} = BMC_{Total} / (A_N + A_S + A_T)$$

where A_N, A_S, and A_T indicate the area (cm^2) of the femoral neck, shaft, and trochanter, respectively.

Moreover, the correlation between BMC_{Total} and BMD_{Total} and the SIeFF of the femoral head (BMC_H and BMD_H), as well as the correlation between BMC_{Total} and BMD_{Total} and the average value of the SIeFF on three sites (femoral neck, shaft, and trochanter) were calculated.

2.7. Statistical analysis

Pearson's correlation coefficient was used to calculate the correlation between SIeFF of bone marrow fat and DXA data (BMD and BMC). *P*-values < 0.05 denoted statistically significant differences.

ImageJ v.1.52 software (National Institutes of Health, Bethesda, Maryland, USA) was used for the measurement of signal intensity, Microsoft Excel (Microsoft, Redmond, WA, USA) was used for arithmetic processing, and EZR version 1.37(Jichi Medical University, Saitama, Japan) [25] was used for the statistical analyses.

3. Results

3.1. Comparison between SIeFF of bone marrow fat and DXA data

The size of the ROI was 832.5 ± 192.6 mm^2 for the right femoral head, 710.4 ± 171.7 mm^2 for the left femoral head, 197.7 ± 60.4 mm^2 for the right femoral neck, 205.9 ± 60.8 mm^2 for the left femoral neck, 158.4 ± 31.3 mm^2 for the right shaft, 147.0 ± 33.9 mm^2 for the left shaft, 169.4 ± 44.7 mm^2 for the right trochanter, and 154.0 ± 26.9 mm^2 for the left trochanter.

According to Pearson's correlation coefficient, the SIeFF and total BMC and BMD showed a strong inverse correlation in the femoral head ($r < -0.74$) and a moderate inverse correlation in the other sites ($r = -0.66$ to -0.45). For almost all combinations, the P-value was < 0.05, except for the right side of BMC_S ($P = 0.07$) and the right side of BMD_T ($P = 0.11$) (Table 1; Figs. 2 and 3).

4. Discussion

In the present study, fat-containing nutritional supplements were used to estimate the amount of fat in the bone. Bone mineral degradation due to aging is caused by mineral loss and fat replacement in the cancellous bone. A decrease in bone component and an increase in fat component have been previously reported [9, 10]. To eliminate device and sequence dependence for this analysis, it was necessary to use a reference material containing fat. Hence, saline, two concentrations (10% and 20%) of an off-the-shelf fat-containing solution, and 100% oil were used for this purpose.

SIeFF was inversely correlated with almost all BMD and BMC when using reference substances, except for a few combinations. In particular, the femoral head and total BMC and BMD were strongly inversely correlated. Since the ROI of the femoral head could be set wider than in other areas, we considered that stable data could be obtained with minimal error due to individual differences. In contrast, it was not possible to evaluate the femoral head using DXA because of the influence of the pelvis. However, although a correlation between BMD, BMC, and SIeFF was observed, it was not strong in all cases. This is probably due to the difference in the observation method; MRI directly observes a cross-sectional section, whereas X-ray examination produces images of three-dimensional material projected and superimposed in two dimensions.

It is not possible to directly account for the third dimension (i.e., depth) because it is in the same direction as the X-ray beam. In BMD measurement, the third dimension is unaccounted for; therefore, problems

with DXA-derived BMD can arise [26, 27]. Therefore, the two-dimensional images provided by DXA do not correspond to the actual volumetric density [26]. Moreover, DXA measurements depend on bone size [28], and do not correspond to the actual volumetric density [26]. Size adjustment determined using predefined indices (e.g., BMD) may fail to fully correct BMC for bone and body size, and may lead to spurious associations with size-related variables [28].

Unlike DXA, MRI can directly evaluate bone morphological information and signal intensities by obtaining cross-sectional images. Through this method, it is possible to evaluate osteoporosis and simultaneously obtain MR images.

Moreover, the apparent volumetric BMD from DXA was moderately correlated with BMD from the size of the lumbar spine measured by MRI [29]. It has also been reported that the fat content can be measured more accurately using T2* [30]. Furthermore, the MRI-derived T2* method may be used to approximate the BMD in the proximal femur [31]. Thus, it may be easier to perform a cross-sectional analysis by MRI than DXA by X-ray examination.

This study had several limitations. Regarding the reasons responsible for the weak correlation between BMD, BMC, and SIeFF, it is unlikely that errors due to sensitivity distribution were caused by the correction for coil sensitivity. This error may have occurred due to the smaller size of the other ROIs compared to the femoral head.

In this study, we only used the two commercially available concentrations of the fat-containing nutrient solution (10% and 20%). Use of a solution with higher fat content (i.e., 20–100%) could have resulted in more accurate measurements. However, if the reference substances were created, uniform and stable emulsification would be required. Moreover, emulsification by mixing additives (e.g., glycerin) would be required. This is a complicated process, which reduces reproducibility. Therefore, we selected an off-the-shelf product that was readily available, safe, and chemically stable. The linearity between fat content (%) and signal intensity has been confirmed beforehand (see 2.3). It is hypothesized that signals generated by fat-containing solutions with concentrations ranging from 20–100% may be used by linear approximation. Therefore, we think that it is possible to calculate the approximate fat content through this approach.

The measured value was set to SIeFF because the reference material contains nonfat components (i.e., glycerin) to prevent separation and is not a pure fat signal. Accordingly, the signal intensity of Intralipos® may include the signal intensity of such additives; however, the effect of these additives on the overall signal intensity of Intralipos® was not confirmed. Moreover, SIeFF was not compared with the fat fraction by other calculation methods, particularly the Dixon method. Furthermore, differences due to varied parameter settings were not examined. However, we considered that the reference data were obtained using the most commonly utilized sequence in routine analyses. Using reference substances in MRI, we were able to propose a reproducible and simple method that could directly acquire cross-sectional information.

Other limitations were the small number of volunteers (especially females) and the lack of different magnetic field strengths. However, it would be useful to show the applicability of SIeFF in low-magnetic field devices. Low-magnetic field devices are often installed in clinics; hence, the availability of such devices would allow health examinations to be performed at the family doctor level without the need to visit a hospital.

In the future, it will be necessary to investigate this method in other regions of the body, such as the lumbar spine. We think that this technique will assist in the examination of osteoporosis in addition to the regular examination. Furthermore, it is important to collect data of patients belonging to different age groups. Through this approach, we could potentially determine the criteria for osteoporosis based on age, as in the dataset produced by the Japanese Society for Bone and Mineral Research 2012 [32]. Therefore, it is desirable to obtain a cutoff value for osteoporosis through the acquisition of a large amount of actual patient data. In addition, the T1-weighted image strongly reflects the fat signal, and is useful for evaluating fat content in the bone; however, noise from sources other than fat may affect the signal intensity. Thus, the relationship between bone mineral and SIeFF of the femoral head showed a strong linearity; however, further study should be needed to make it a surrogate for DXA.

5. Conclusion

Commercially available fat-containing agents may be useful in estimating the bone marrow fat content for bone mineral measurement by MRI. The SIeFF, BMC, and BMD showed a strong inverse correlation in the femoral head. However, a more thorough study is warranted before this method can be used as an alternative to DXA.

Declarations

Acknowledgments

The authors would like to thank Mr. Koji Uchida in Center for Information and Neural Networks National Institute of Information and Communications Technology, Dr. Shunichi Motegi in Gunma Paz University and Dr. Rei Yoshida in Kurihara Central Hospital for his valuable advice and technical support on measurements.

Funding: The authors declare that no funds, grants, or other support were received during the preparation of this manuscript.

Conflict of Interest: The authors declares that he/she has no conflict of interest.

Ethical approval: All procedures performed in studies involving human participants were in accordance with the ethical standards of the institutional and/or national research committee and with the 1964 Helsinki declaration and its later amendments or comparable ethical standards.

Informed consent: Informed consent was obtained from all individual participants included in the study.

Competing Interests

The authors have no relevant financial interests and non-financial interests to disclose.

Author Contributions

All author contributed to the study conception and design. Material preparation and data collection were performed by Yasuo Takatsu, Yuriko Nohara, Kenichiro Yamamura, and Kunihiro Yabe. Analysis was performed by Yasuo Takatsu and Tomoko Takeyama. This study was supervised by Tosiaki Miyati. The first draft of the manuscript was written by Yasuo Takatsu, and all authors commented on previous version of the manuscript. All authors read and approved the final manuscript.

Consent to publish

All volunteers provided written informed consent for their participation in this study.

References

1. Cummings SR, Black D (1995) Bone mass measurements and risk of fracture in Caucasian women: a review of findings from prospective studies. Am J Med 98:24S–28S. https://doi.org/10.1016/s0002-9343(05)80041-5.
2. Pietschmann P, Rauner M, Sipos W, Kerschan-Schindl K (2009) Osteoporosis: an age-related and gender-specific disease–a mini-review. Gerontology 55:3-12. https://doi.org/10.1159/000166209.
3. Hofbauer LC, Brueck CC, Singh SK, Dobnig H (2007) Review Osteoporosis in Patients with Diabetes Mellitus. J Bone Miner Res 22:1317-1328. https://doi.org/10.1359/jbmr.070510.
4. Zhao LJ, Jiang H, Papasian CJ, Maulik D, Dress B, Hamilton J, Deng HW (2008) Review Correlation of Obesity and Osteoporosis: Effect of Fat Mass on the Determination of Osteoporosis. J Bone Miner Res 23:17-29. https://doi.org/10.1359/jbmr.070813
5. Hu L, Yin C, Zhao F, Ali A, Ma J, Qian A (2018) Mesenchymal Stem Cells: Cell Fate Decision to Osteoblast or Adipocyte and Application in Osteoporosis Treatment. Int J Mol Sci 19:360. https://doi.org/10.3390/ijms19020360.
6. Hwang DK, Choi HJ (2010) The relationship between low bone mass and metabolic syndrome in Korean women. Osteoporos Int 21:425–431. https://doi.org/10.1007/s00198-009-0990-2.
7. Blaauw R, Albertse EC, Hough S (1996) Body fat distribution as a risk factor for osteoporosis. S Afr Med J86:1081–1084.
8. von Muhlen D, Safii S, Jassal SK, Svartberg J, Barrett-Connor E (2007) Associations between the metabolic syndrome and bone health in older men and women: the Rancho Bernardo Study. Osteoporos Int 18:1337–1344. https://doi.org/10.1007/s00198-007-0385-1.

9. Paccou J, Hardouin P, Cotten A, Penel G, Cortet B (2015) The role of bone marrow fat in skeletal health: usefulness and perspectives for clinicians. J Clin Endocrinol Metab.;100:3613–3621. https://doi.org/10.1210/jc.2015-2338.
10. Baum T, Yap SP, Karampinos DC, Nardo L, Kuo D, Burghardt AJ, Masharani UB, Schwartz AV, Li X, Link TM (2012) Does vertebral bone marrow fat content correlate with abdominal adipose tissue, lumbar spine BMD and blood biomarkers in women with type 2 diabetes mellitus? J Magn Reson Imaging 35:117–124. https://doi.org/10.1002/jmri.22757.
11. WHO study group (1994) Assessment of fracture risk and its application to screening for postmenopausal osteoporosis. WHO technical report series 843, Geneva, Switzland.
12. Bredella MA, Daley SM, Kalra MK, Keenan BJ, Miller KK, Torriani M (2015) Marrow adipose tissue quantification of the lumbar spine by using dual-energy CT and single-voxel (1)H MR spectroscopy: a feasibility study. Radiology 277:230–235. https://doi.org/10.1148/radiol.2015142876
13. Chang JS, Taouli B, Salibi N, Hecht EM, Chin DG, Lee VS (2006) Opposed-phase MRI for fat quantification in fat-water phantoms with 1H MR spectroscopy to resolve ambiguity of fat or water dominance. AJR Am J Roentgenol 187:W103–106. https://doi.org/10.2214/AJR.05.0695.
14. Zhang L, Li S, Hao S, Yuan Z (2016) Quantification of fat deposition in bone marrow in the lumbar vertebra by proton MRS and in-phase and out-of-phase MRI for the diagnosis of osteoporosis. J Xray Sci Technol 24:257–266. https://doi.org/10.3233/XST-160549.
15. Cordes C, Baum T, Dieckmeyer M, Ruschke S, Diefenback MN, Hauner H, Kirschke JS, Karampinos DC (2016) MR-based assessment of bone marrow fat in osteoporosis, diabetes, and obesity. Front Endocrinol (Lausanne) 7:74. https://doi.org/10.3389/fendo.2016.00074.
16. Zhang Y, Zhou Z, Wang C, Cheng X , Wang L, Duanmu Y, Zhang C, Veronese N, Guglielmi G (2018) Reliability of measuring the fat content of the lumbar vertebral marrow and paraspinal muscles using MRI mDIXON-Quant sequence. Diagn Interv Radiol 24:302–307. https://doi.org/10.5152/dir.2018.17323.
17. Loau J, Shiehmorteza M, Girard OM, Sirlin CB, Bydder M (2013) Evaluation of MRI fat fraction in the liver and spine pre and post SPIO infusion. Magn Reson Imaging 31:1012-1016. https://doi.org/10.1016/j.mri.2013.01.016.
18. Fishbein MH, Gardner KG, Potter CJ, Schmalbrock P, Smith MA (1997) Introduction of fast MR imaging in the assessment of hepatic steatosis. Magn Reson Imaging 15:287–293. https://doi.org/10.1016/s0730-725x(96)00224-x.
19. Sane S, Baba M, Kusano C, Shirao K, Kamada T, AikouT (1999) Fat emulsion administration in the early postoperative period in patients undergoing esophagectomy for carcinoma depresses arachidonic acid metabolism in neutrophils. Nutrition 15:341-346. https://doi.org/10.1016/s0899-9007(99)00032-5.
20. Hoshino R, Kamiya Y, Fujii Y, Ttsubokawa T (2017) Lipid emulsion injection-induced reversal of cardiac toxicity and acceleration of emergence from general anesthesia after scalp infiltration of a local anesthetic: a case report. JA Clin Rep 3:9. https://doi.org/10.1186/s40981-017-0077-6.

21. Peterson P, Svensson J, Månsson S (2014) Relaxation Effects in MRI-Based Quantification of Fat Content and Fatty Acid Composition. Magn Reason Med.72:1320-1329. https://doi.org/10.1002/mrm.25048.
22. Mashhood A, Railkar R, Yokoo T, Levin Y, Clark L, Fox-Bosetti S, Middleton MS, Riek J, Kauh E, Dardzinski BJ, Williams D, Sirlin C, Shire NJ (2013) Reproducibility of Hepatic Fat Fraction Measurement by Magnetic Resonance Imaging. J Magn Reason Imaging 37:1359-1370. https://doi.org/10.1002/jmri.23928.
23. Japan osteoporosis society, bone strength evaluation committee (2007) Proximal femur BMD measurement manual (in Japanese). Osteoporosis Japan 15:1–41.
24. Pellegrino F, Zatelli MC, Bondanelli M, Carnevale A, Cittanti C, Fortini M, Gamberini MR, Giganti M, Ambrosio MR (2019) Dual-energy X-ray absorptiometry pitfalls in Thalassemea Major. Endocrine 65:469–482. https://doi.org/10.1007/s12020-019-02003-x.
25. Kanda Y (2013) Investigation of the freely available easy-to-use software 'EZR' for medical statistics. Bone Marrow Transplant 48:452–458. https://doi.org/10.1038/bmt.2012.244.
26. Binkovitz LA, Henwood MJ (2007) Pediatric DXA: technique and interpretation. Pediatr Radiol 37: 21–31. https://doi.org/10.1007/s00247-006-0153-y.
27. Carter DR, Bouxsein ML, Marcus R (1992) New approaches for interpreting projected bone densitometry data. J Bone Miner Res 7:137–145. https://doi.org/10.1002/jbmr.5650070204.
28. Prentice A, Parsons TJ, Cole TJ (1994) Uncritical use of bone mineral density in absorptiometry may lead to size- related artifacts in the identification of bone mineral determinants. Am J Clin Nutr 60:837–842. https://doi.org/10.1093/ajcn/60.6.837
29. Kröger H, Vainio P, Nieminen J, Kotaniemi A (1995) Comparison of different models for interpreting bone mineral density measurements using DXA and MRI technology. Bone 17:157–159. https://doi.org/10.1016/s8756-3282(95)00162-x.
30. Arai N, Miyati T, Matsunaga S, Motono Y, Ueda Y, Kasai H, Suzuki Y, Matsuda T (2007) New method of determining regional fat fraction with modulus and real multiple gradient-echo (MRM-GRE). Nihon Hoshasen Gijutsu Gakkai Zasshi (in Japanese) 63:312–318. https://doi.org/10.6009/jjrt.63.312
31. Arokoski MH, Arokoski JPA, Vainio P, Niemitukia LH, Kröger H, Jurvelin JS (2002) Comparison of DXA and MRI methods for interpreting femoral neck bone mineral density. J Clin Densitom 5:289–296. https://doi.org/10.1385/jcd:5:3:289.
32. Seon S, Fukunaga M, Sugimoto T, Sone T, Fujiwara S, Endo N, Gorai I, Shiraki M, Hagino H, Hosoi T, Ohta H, Yoneda T, Tomomitsu T; Japanese Society for Bone and Mineral Research and Japan Osteoporosis Society Joint Review Committee for the Revision of the Diagnostic Criteria for Primary Osteoporosis (2013) Diagnostic criteria for primary osteoporosis: year 2012 revision. J Bone Miner Metab 31:247–257. https://doi.org/10.1007/s00774-013-0447-8.

Tables

Table 1 Correlation between BMC, BMD and SIeFF (%)

Position	R/L	SIeFF (%); mean ± SD	BMC (g)			BMD (g/cm^2)		
			r	CI 95%	*P* value	*r*	CI 95%	*P* value
Femoral Head-Total	R	56.19 ± 10.52	-0.74	-0.91 – -0.34	<0.01	-0.76	-0.92 – -0.39	<0.01
	L	54.91 ± 9.35	-0.82	-0.94 – -0.52	<0.01	-0.78	-0.93 – -0.43	<0.01
Femoral Neck	R	60.87 ± 12.30	-0.56	-0.84 – -0.04	<0.05	-0.66	-0.88 – -0.20	<0.01
	L	62.97 ± 13.40	-0.59	-0.85 – -0.08	<0.05	-0.60	-0.86 – -0.10	<0.05
Shaft	R	60.92 ± 12.39	-0.50	-0.81 – 0.05	0.07	-0.63	-0.87 – -0.15	<0.05
	L	63.96 ± 13.16	-0.55	-0.84 – -0.02	<0.05	-0.55	-0.83 – -0.02	<0.05
Trochanter	R	64.18 ± 9.35	-0.56	-0.84 – -0.04	<0.05	-0.45	-0.79 – 0.11	0.11
	L	70.91 ± 8.42	-0.57	-0.84 – -0.05	<0.05	-0.67	-0.89 – -0.21	<0.01
Average-Total	R	61.99 ± 10.77	-0.64	-0.85 – -0.07	<0.05	-0.58	-0.88 – -0.17	<0.05
	L	65.95 ± 10.59	-0.59	-0.85 – -0.08	<0.05	-0.66	-0.88 – -0.20	<0.05

Average, average value of SIeFF for the total proximal femur (femoral neck, shaft, and trochanter); BMC, bone mineral content (g); BMD, bone mineral density (g / cm^2); CI 95%, 95% confidence interval; L, left side; *r*, Pearson product-moment correlation coefficient; R, right side; SD, standard deviation; SIeFF, signal intensity based on the estimated fat fraction using magnetic resonance imaging; Total, value of the total proximal femur (femoral neck, shaft, and trochanter) using the dual-energy-X-ray-absorptiometry

Figures

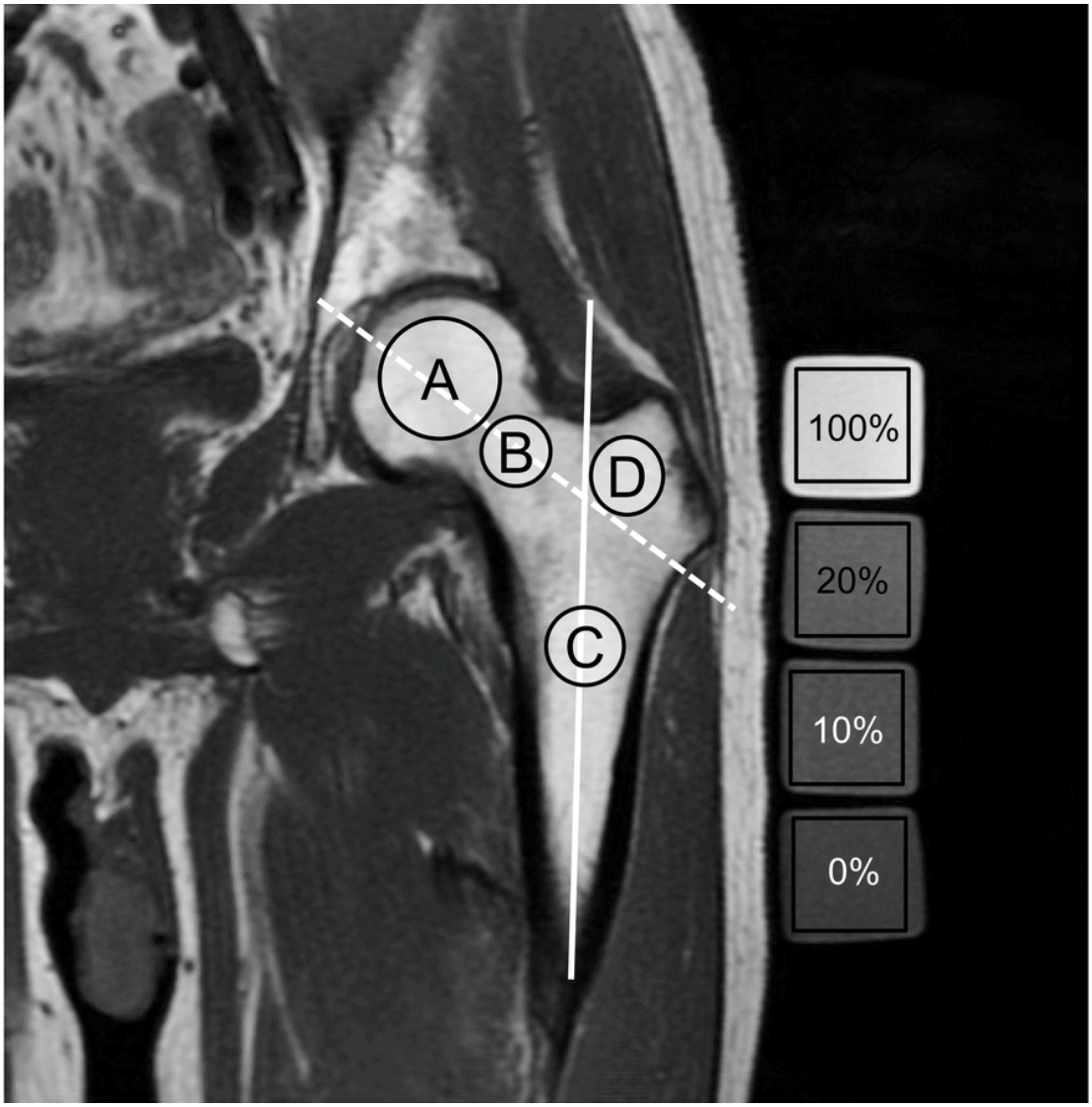

Figure 1

Selection of the region of interest (ROI)

(A) Femoral head. (B) Femoral neck. (C) Shaft. (D) Trochanter.

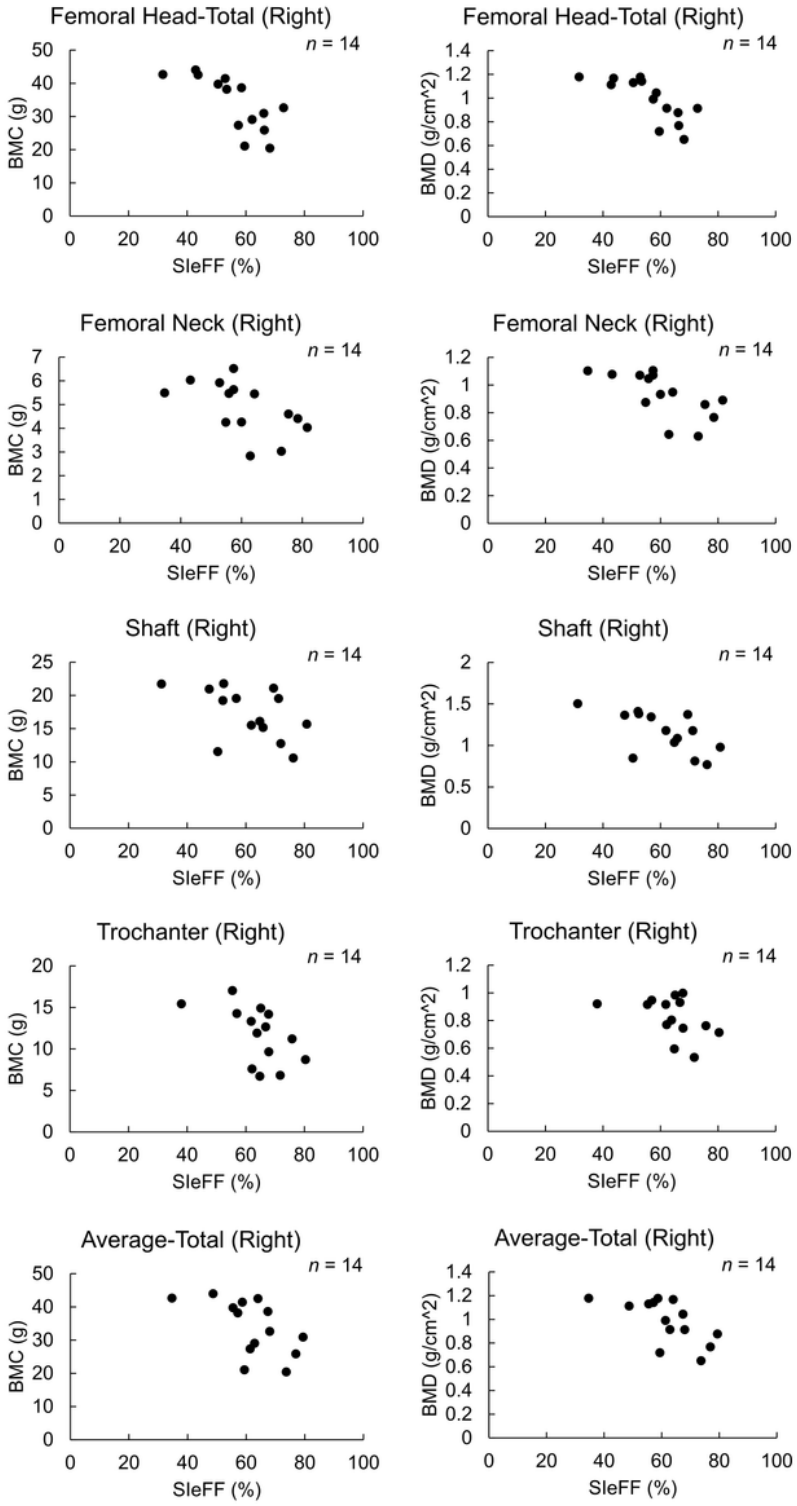

Figure 2

Correlations between BMC, BMD, and SIeFF (%) in the right femur

BMC, bone mineral content; BMD, bone mineral density; SIeFF, estimated fat fraction based on signal intensity.

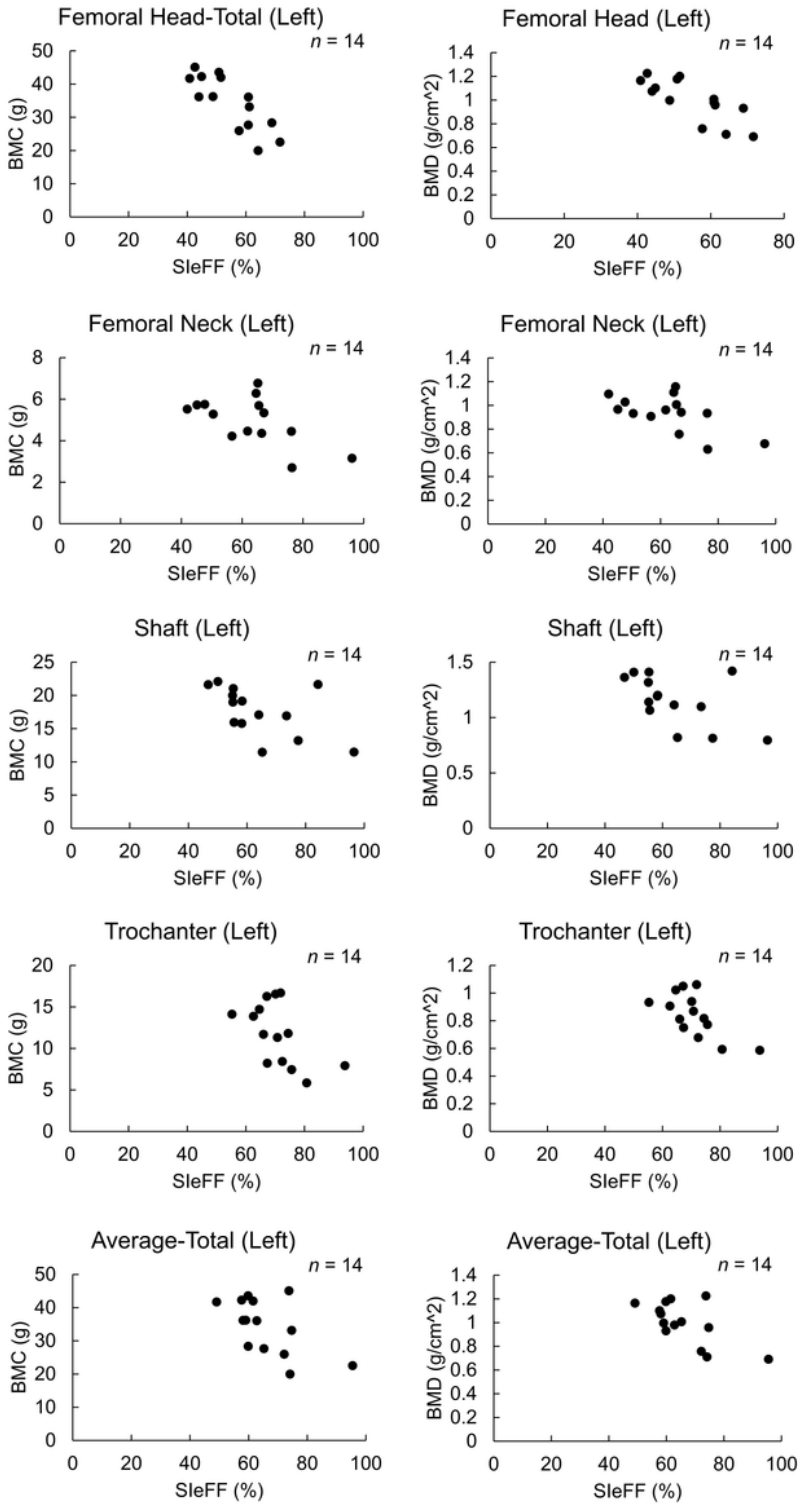

Figure 3

Correlations between BMC, BMD, and SIeFF (%) in the left femur

BMC, bone mineral content; BMD, bone mineral density; SIeFF, estimated fat fraction based on signal intensity.